Optimum Monte Carlo simulations: some exact results

2003 J. Phys. A: Math. Gen. 36 9009

(http://iopscience.iop.org/0305-4470/36/34/305)

INSTITUTE OF PHYSICS PUBLISHING JOURNAL OF PHYSICS A: MATHEMATICAL AND GENERAL

J. Phys. A: Math. Gen. **36** (2003) 9009–9023 PII: S0305-4470(03)59491-4

Optimum Monte Carlo simulations: some exact results

J Talbot[1], **G Tarjus**[2] **and P Viot**[2]

[1] Department of Chemistry and Biochemistry, Duquesne University, Pittsburgh, PA 15282-1530, USA
[2] Laboratoire de Physique Théorique des Liquides, Université Pierre et Marie Curie, 4, place Jussieu, 75252 Paris Cedex, 05, France

Received 7 February 2003, in final form 9 July 2003
Published 12 August 2003
Online at stacks.iop.org/JPhysA/36/9009

Abstract
We obtain exact results for the acceptance ratio and mean squared displacement in Monte Carlo simulations of the simple harmonic oscillator in D dimensions. When the trial displacement is made uniformly in the radius, we demonstrate that the results are independent of the dimensionality of the space. We also study the dynamics of the process via a spectral analysis and obtain an accurate description for the relaxation time.

PACS numbers: 05.70.Ln, 81.05.Rm, 75.10.Nr, 64.60.My, 68.43.Mn, 75.40.Gb

1. Introduction

Since the original Metropolis algorithm appeared five decades ago, countless studies have employed the technique to evaluate the thermodynamic properties of model systems (Allen and Tildesley 1987, Binder 1997, Frenkel and Smit 2002). The essence of the method is to generate a sequence of configurations that represent a given thermodynamic ensemble, often the canonical ensemble. Properties of interest are then obtained as averages over the configurations. At each step of the simulation a trial configuration is obtained from the current one by making a random displacement in the configuration space. This might correspond to, for example, displacing a randomly selected particle. The trial configuration is either accepted or rejected with a probability given by the appropriate Boltzmann factor for the ensemble. In case of rejection, the current configuration is retained for use in evaluating the properties of interest.

Since many applications of MC are computationally intensive, a much addressed issue has been the optimization of the simulation with respect to one or more control parameters so that the configuration space is sampled in the most efficient way. Bouzida, Kumar and Swendsen (BKS) (Bouzida *et al* 1992, Swendsen 2002), as part of a programme aimed at improving the efficiency of MC simulations of biomolecules, performed numerical studies of the simple harmonic oscillator (SHO) where the convergence of the simulation depends on

the maximum displacement. There is no unique measure of efficiency, but two simple choices are the mean squared and mean absolute displacements. As the maximum displacement tends to zero or infinity it is clear that the average value of both of these quantities tends to zero since, in the first case the particle does not move, while in the second all attempted moves are rejected. Thus both quantities have a maximum for some intermediate value of the maximum displacement.

It is also useful to consider the dynamical process associated with an MC simulation, even though it does not correspond to the actual dynamics of the system. One can, for example, calculate various time correlation functions that can be used to develop alternative efficiency criteria (Kolafa 1988, Mountain and Thirumalai 1994).

BKS (Bouzida *et al* 1992) performed numerical studies of the SHO in one, two and three dimensions and examined the acceptance ratio $P_{\rm acc}$ (i.e., the fraction of accepted trial configurations), mean squared, $\langle(\Delta x)^2\rangle$, and mean absolute, $\langle|\Delta x|\rangle$, displacements as a function of the maximum displacement, δ. They found that the acceptance ratio decreases approximately exponentially for small to intermediate values of δ and then inversely for larger values. In one dimension they found that the maxima in $\langle(\Delta x)^2\rangle$ and $\langle|\Delta x|\rangle$ occur at $P_{\rm acc} = 0.42$ and $P_{\rm acc} = 0.56$, respectively[3]. In higher dimensions the results depend on how the jump is made. BKS considered two cases: in one the jumps are performed uniformly to any point in a spherical volume of radius δ centred on the current position, a choice that favours larger radial displacements for dimensions $D > 1$. In a second method, the jumps were sampled uniformly in the radius (and randomly in the orientation) so that all radial displacements are equally probable. In the former case BKS observed that, for a given δ, $P_{\rm acc}$ decreases as a function of D, while for uniform radius sampling the numerical results suggested that $P_{\rm acc}$ is independent of D.

In addition to these static properties, BKS also examined the correlation time, τ, of the energy–energy correlation function. They observed a minimum correlation time for an acceptance ratio of approximately 50%.

Here we present an analytical study of the SHO in arbitrary dimension. We obtain exact expressions for the acceptance ratio and the mean squared and mean absolute displacements as functions of the maximum displacement δ. We show that when the trial jump is selected uniformly in the radius, the results are independent of the dimension. We also present an analysis of the dynamics of the process.

2. One dimension

We first investigate the case of a SHO in one dimension, whose potential energy is given by $V(x) = kx^2/2$ where x is the position and k is the stiffness constant.

In a standard Metropolis Monte Carlo simulation one makes a trial move with a uniform random displacement selected between $-\delta$ and δ. The dynamical process generated by the successive trial moves of the Monte Carlo simulation can be written as

$$\frac{{\rm d}P(x,t)}{{\rm d}t} = -\frac{1}{2\delta}\int_{-\delta}^{\delta} {\rm d}h\, W(x \to x+h)P(x,t) + \frac{1}{2\delta}\int_{-\delta}^{\delta} {\rm d}h\, W(x+h \to x)P(x+h,t) \qquad (1)$$

[3] Figures 1 and 2 of (Bouzida *et al* 1992) indicate that the authors were in possession of an analytical expression for the probability versus displacement, as well as other static quantities, in the one-dimensional system. However, no formulae are given and there is no discussion of how the results were obtained.

where $W(x \to x+h)$ denotes the transition rate from the state x to the state $x+h$ and $P(x,t)$ is the probability of finding the oscillator at position x at time t. To ensure the convergence towards equilibrium, a sufficient condition is given by detailed balance, which is expressed as

$$\frac{W(x \to x+h)}{W(x+h \to x)} = \frac{P_{\rm eq}(x+h)}{P_{\rm eq}(x)} \tag{2}$$

where

$$P_{\rm eq}(x) = c \exp(-\beta V(x)) \tag{3}$$

and $c = \sqrt{\beta k/2\pi}$ is a normalization constant ensuring that $\int_{-\infty}^{\infty} {\rm d}x\, P_{\rm eq}(x) = 1$. One solution of equation (2) is the Metropolis rule,

$$W(x \to x+h) = \min(1, \exp(-\beta(V(x+h) - V(x))). \tag{4}$$

Most of the properties of the 1D SHO can be obtained analytically. For instance, the acceptance ratio, which is the number of accepted trials over the total number of trials can be expressed as

$$P_{\rm acc}(\delta) = c \int_{-\infty}^{+\infty} {\rm d}x\, {\rm e}^{-\beta V(x)} \frac{1}{2\delta} \int_{-\delta}^{\delta} {\rm d}h\, W(x \to x+h). \tag{5}$$

In this equation $\exp(-\beta V(x))\,{\rm d}x$ is the probability that the oscillator is between x and $x+{\rm d}x$, ${\rm d}h/2\delta$ is the probability of selecting a random displacement between h and $h+{\rm d}h$ and $W(x \to x+h)$ is the probability of accepting the trial displacement (given by equation (4)). Integration over the allowed values of x and h then gives the average acceptance probability. Since displacements to the left and right are symmetric, we need to consider only one direction. For displacements to the right, equation (5) can be written as

$$\frac{{\rm d}(\delta P_{\rm acc}(\delta))}{{\rm d}\delta} = c \int_{-\infty}^{+\infty} {\rm d}x\, {\rm e}^{-\beta V(x)} W(x \to x+\delta). \tag{6}$$

For $x < -\delta/2$, $W(x \to x+\delta) = 1$ and for $x > -\delta/2$, $W(x \to x+\delta) = {\rm e}^{-\beta k((x+\delta)^2 - x^2)/2}$. One thus obtains

$$\frac{{\rm d}(\xi P_{\rm acc}(\xi))}{{\rm d}\xi} = 1 - {\rm erf}\left(\frac{\xi}{2}\right) \tag{7}$$

where ${\rm erf}(x)$ is the error function and $\xi = \sqrt{\frac{\beta k}{2}}\delta$. Using the initial condition, i.e., $P_{\rm acc}(0) = 1$, the solution of the differential equation (7) is

$$P_{\rm acc}(\xi) = 1 - {\rm erf}\left(\frac{\xi}{2}\right) + \frac{2}{\sqrt{\pi}\xi}(1 - {\rm e}^{-\xi^2/4}). \tag{8}$$

The function is plotted in figure 1.

The mean squared displacement, $\langle(\Delta x)^2\rangle$, and the mean absolute displacement, $\langle|\Delta x|\rangle$, defined as

$$\langle(\Delta x)^2\rangle = c \int_{-\infty}^{+\infty} {\rm d}x \exp(-\beta V(x)) \frac{1}{2\delta} \int_{-\delta}^{\delta} {\rm d}h\, h^2 W(x \to x+h) \tag{9}$$

$$\langle|\Delta x|\rangle = c \int_{-\infty}^{+\infty} {\rm d}x \exp(-\beta V(x)) \frac{1}{2\delta} \int_{-\delta}^{\delta} {\rm d}h |h| W(x \to x+h) \tag{10}$$

can be quite simply obtained from the generating function

$$Z(\lambda) = c \int_{-\infty}^{+\infty} {\rm d}x \exp(-\beta V(x)) \frac{1}{2\delta} \int_{-\delta}^{\delta} {\rm d}h \exp(-\lambda|h|) W(x \to x+h) \tag{11}$$

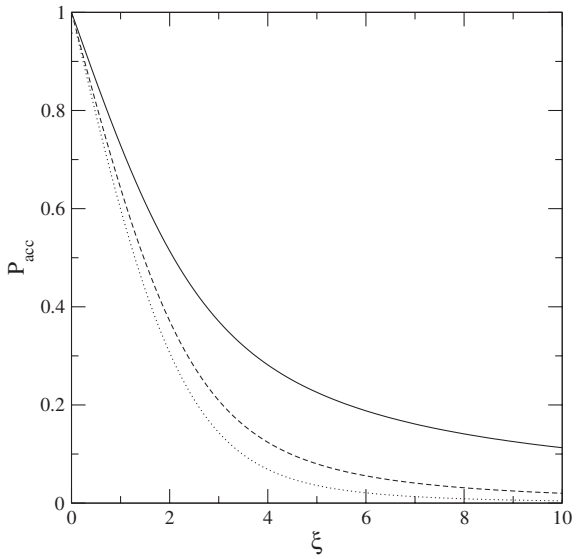

Figure 1. Acceptance ratio $P_{\rm acc}$ versus $\xi = \sqrt{\frac{\beta k}{2}}\delta$ for a harmonic oscillator with uniform volume sampling in $D = 1$, 2 and 3 dimensions (full, dashed and dotted lines respectively). For a uniform radius sampling, all curves coincide with the one-dimensional result (full line).

by the derivatives with respect to λ and set $\lambda = 0$, i.e., $\langle|\Delta x|\rangle = -(\partial Z(\lambda)/\partial\lambda)_{\lambda=0}$, $\langle(\Delta x)^2\rangle = (\partial^2 Z(\lambda)/\partial\lambda^2)_{\lambda=0}$ (and, of course, $P_{\rm acc} = Z(\lambda = 0)$).

By multiplying both sides of equation (11) by ξ and next differentiating with respect to ξ, one obtains

$$\frac{\partial(\xi Z(\lambda,\xi))}{\partial\xi} = \exp\left(-\sqrt{\frac{2}{\beta k}}\lambda\xi\right)\left(1 - \mathrm{erf}\left(\frac{\xi}{2}\right)\right) \tag{12}$$

which, after defining $\tilde{\lambda} = \sqrt{\frac{2}{\beta k}}\lambda$, leads to

$$Z(\lambda,\xi) = \frac{1}{\tilde{\lambda}\xi}\left[1 - \exp(-\tilde{\lambda}\xi)\left(1 - \mathrm{erf}\left(\frac{\xi}{2}\right)\right) - \exp(\tilde{\lambda}^2)\left(\mathrm{erf}\left(\frac{\xi}{2} + \tilde{\lambda}\right) - \mathrm{erf}(\tilde{\lambda})\right)\right]. \tag{13}$$

By taking the derivatives of the above formula with respect to λ and evaluating the resulting expressions at $\lambda = 0$, it is easy to show that the mean squared and mean absolute displacements are given by

$$\sqrt{\frac{\beta k}{2}}\langle|\Delta x|\rangle = \left[\frac{\xi}{2}\left(1 - \mathrm{erf}\left(\frac{\xi}{2}\right)\right) - \frac{1}{\sqrt{\pi}}\exp\left(-\frac{\xi^2}{4}\right) + \frac{\mathrm{erf}\left(\frac{\xi}{2}\right)}{\xi}\right] \tag{14}$$

$$\frac{\beta k}{2}\langle(\Delta x)^2\rangle = \frac{1}{3}\left[\xi^2\left(1 - \mathrm{erf}\left(\frac{\xi}{2}\right)\right) + \frac{8}{\sqrt{\pi}\xi}\left(1 - \left(1 + \frac{\xi^2}{4}\right)\exp\left(-\frac{\xi^2}{4}\right)\right)\right]. \tag{15}$$

The maximum in the mean squared and mean absolute displacements occur for $\xi = 2.616\,48$ and $\xi = 1.763\,32$, which corresponds to acceptance ratio values of $P_{\rm acc} = 0.417\,67$ and $P_{\rm acc} = 0.558\,239$ in agreement with the numerical results of BKS (Bouzida *et al* 1992) (see figures 2 and 3).

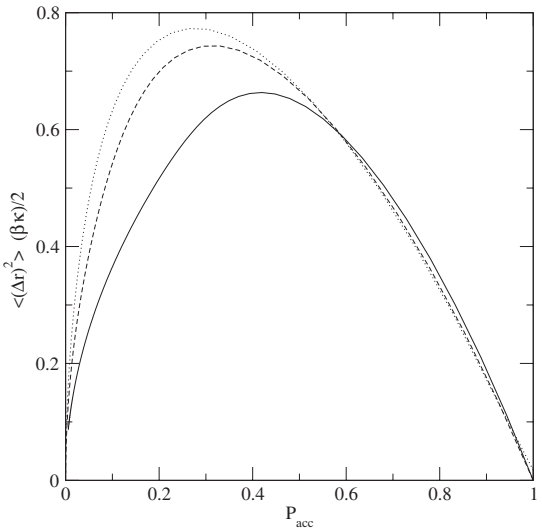

Figure 2. Mean squared displacement $\langle(\Delta r)^2\rangle \frac{\beta k}{2}$ versus the acceptance ratio $P_{\rm acc}$ for uniform volume sampling in one, two and three dimensions (full curve, dashed and dotted lines, respectively). For a uniform radius sampling all curves coincide with the one-dimensional result (full line).

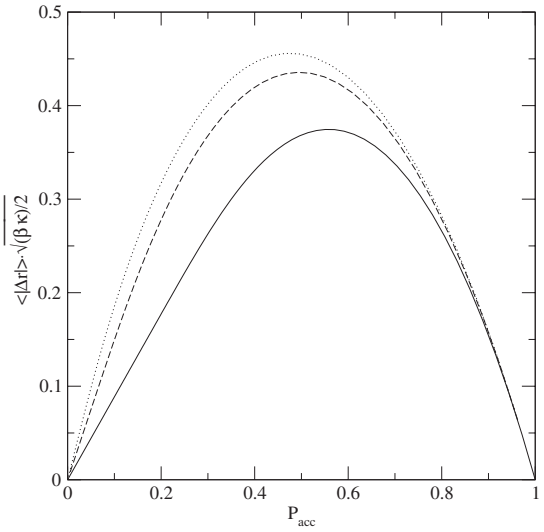

Figure 3. Mean absolute displacement $\langle|\Delta r|\rangle\sqrt{\frac{\beta k}{2}}$ versus the acceptance ratio $P_{\rm acc}$ for a uniform volume sampling in one, two and three dimensions (full curve, dashed and dotted lines, respectively). For a uniform radius sampling all curves coincide with the one-dimensional result (full line).

3. *D* dimensions

We show here that the acceptance ratio, mean squared displacement and other quantities of interest can be obtained exactly in any dimension. Note that the term 'volume' should be

interpreted as the hypervolume in D dimensions, e.g., area in 2D and volume in 3D. For simplicity, we derive exact expressions in odd dimensions, but similar results can be obtained in even dimensions.

3.1. Uniform volume sampling

In D dimensions, the acceptance ratio is expressed as

$$P_{\mathrm{acc}}(\delta) = \frac{c_D}{\delta^D V_D} \int \mathrm{d}^D\mathbf{r} \exp(-\beta k r^2/2) \int_{|h|\leqslant\delta} \mathrm{d}^D\mathbf{h} \min(1, \exp(-\beta k(|\mathbf{r}+\mathbf{h}|^2 - r^2)/2)) \quad (16)$$

where $V_D = \pi^{D/2}/\,\Gamma(D/2+1)$ is the volume of the sphere of unit radius in D dimensions and

$$c_D = \left(D V_D \int_0^\infty \mathrm{d}r r^{D-1} \mathrm{e}^{-\beta k r^2/2} \right)^{-1} = \left(\frac{\beta k}{2\pi} \right)^{D/2}. \quad (17)$$

In odd dimensions, the derivative of equation (16) with respect to δ can be written explicitly by using generalized spherical coordinates

$$\begin{aligned} \frac{\mathrm{d}(\delta^D P_{\mathrm{acc}}(\delta))}{\mathrm{d}\delta} &= \frac{c_D}{V_D} \int \mathrm{d}^D\mathbf{r} \exp(-\beta k r^2/2) \\ &\quad \times \delta^{D-1} \int \mathrm{d}\Omega \min(1, \exp(-\beta k(r\delta\cos\phi_1 + \delta^2/2))) \end{aligned} \quad (18)$$

where $\mathrm{d}\Omega = \left(\prod_{j=1}^{D-2} (\sin(\phi_j))^{D-1-j}\, \mathrm{d}\phi_j\right) \mathrm{d}\phi_{D-1}$ such that $\int \mathrm{d}\Omega = D V_D$. The first $D-2$ variables ϕ_j are integrated from 0 to π, whereas ϕ_{D-1} is integrated from 0 to 2π. If we denote $u = \cos(\phi_1)$, perform integration over $\phi_2 \ldots \phi_{D-1}$ and introduce the variable $v = r\sqrt{\frac{\beta k}{2}}$ equation (18) can be rewritten as

$$\begin{aligned} \frac{\mathrm{d}(\xi^D P_{\mathrm{acc}}(\xi))}{\mathrm{d}\xi} &= D\xi^{D-1} \frac{2}{\Gamma\left(\frac{D}{2}\right) \int_{-1}^1 \mathrm{d}u (1-u^2)^{(D-3)/2}} \\ &\quad \times \int_0^{+\infty} v^{D-1} \mathrm{d}v\, \mathrm{e}^{-v^2} \int_{-1}^1 \mathrm{d}u (1-u^2)^{(D-3)/2} \min(1, \exp(-(2\xi v u + \xi^2))) \end{aligned} \quad (19)$$

where $\min(1, \exp(-(2\xi v u + \xi^2))) = \exp((-(2\xi v u + \xi^2))$ for $v < \xi/2$ with $-1 < u < 1$ and for $v > \xi/2$ with $-\xi/(2v) < u < 1$ and $\min(1, \exp(-(2\xi v u + \xi^2))) = 1$ for $r > \xi/2$ with $-1 < u < -\xi/(2v)$. Using that $\int_{-1}^1 \mathrm{d}u (1-u^2)^{(D-3)/2} = \frac{\Gamma\left(\frac{D-1}{2}\right)}{\Gamma\left(\frac{D}{2}\right)}\sqrt{\pi}$, equation (19) then becomes

$$\begin{aligned} \frac{\mathrm{d}(\xi^D P_{\mathrm{acc}}(\xi))}{\mathrm{d}\xi} &= \frac{2D\xi^{D-1}}{\sqrt{\pi}\,\Gamma\left(\frac{(D-1)}{2}\right)} \left(\int_0^{\xi/2} \mathrm{d}v\, v^{D-1}\, \mathrm{e}^{-v^2} \int_{-1}^1 \mathrm{d}u (1-u^2)^{(D-3)/2} \exp(-(\xi^2 + 2\xi v u)) \right. \\ &\quad + \int_{\xi/2}^{+\infty} v^{D-1} \mathrm{d}v\, \mathrm{e}^{-v^2} \left[\int_{-1}^{-\xi/(2v)} \mathrm{d}u (1-u^2)^{(D-3)/2} \right. \\ &\quad \left. \left. + \int_{-\xi/(2v)}^1 \mathrm{d}u (1-u^2)^{1/2} \exp((-(\xi^2 + 2\xi v u))) \right] \right). \end{aligned} \quad (20)$$

After some calculation (see appendix A) one obtains

$$\frac{\mathrm{d}(\xi^D P_{\mathrm{acc}}(\xi))}{\mathrm{d}\xi} = D\xi^{D-1} \left(1 - \mathrm{erf}\left(\frac{\xi}{2} \right) \right) \quad (21)$$

which gives, for instance, in three dimensions

$$P_{\rm acc}(\xi) = 1 - \mathrm{erf}\left(\frac{\xi}{2}\right) + \frac{8}{\sqrt{\pi}\xi^3}\left(1 - \left(1 + \frac{\xi^2}{4}\right)\exp\left(-\frac{\xi^2}{4}\right)\right). \tag{22}$$

Figure 1 shows the acceptance ratio $P_{\rm acc}$ versus δ in one, two and three dimensions.

A similar calculation for generating function $Z_D(\lambda, \xi)$ leads to

$$\frac{\partial(\xi^D Z_D(\tilde{\lambda}, \xi))}{\partial \xi} = D\xi^{D-1}\mathrm{e}^{-\tilde{\lambda}\xi}\left(1 - \mathrm{erf}\left(\frac{\xi}{2}\right)\right) \tag{23}$$

and to

$$Z_D(\tilde{\lambda}, \xi) = D(-\xi)^{1-D}\frac{\partial^{D-1}}{\partial \tilde{\lambda}^{D-1}} Z_{D=1}(\tilde{\lambda}, \xi) \tag{24}$$

where the expression for $Z_{D=1}(\tilde{\lambda}, \xi)$ is given in equation (13). Since $P_{\rm acc}(\xi) = Z_D(\tilde{\lambda} = 0, \xi)$, it follows from equation (24) that the acceptance ratio in D dimensions is equal, up a factor $D(-\xi)^{1-D}\sqrt{\frac{\beta k}{2}}$, to the mean squared displacement $\langle(\Delta x)^2\rangle$ in one dimension: compare equation (22) to equation (15).

Although straightforward, the algebra rapidly becomes tedious, and we only illustrate the results by giving the expression of the mean squared displacement $\langle(\Delta r)^2\rangle$ in three dimensions

$$\begin{aligned}\frac{\beta k}{2}\langle(\Delta r)^2\rangle &= \frac{\partial^2}{\partial \tilde{\lambda}^2} Z_{D=3}(\tilde{\lambda}, \xi)|_{\tilde{\lambda}=0} \\ &= \frac{3}{\xi^2}\left(\frac{\beta k}{2}\right)^2 \langle(\Delta x)^4\rangle_{D=1} \\ &= \frac{12}{5}\left[\frac{\xi^2}{4}\left(1 - \mathrm{erf}\left(\frac{\xi}{2}\right)\right) + \frac{16}{\sqrt{\pi}\xi^2}\left(1 - \left(1 + \frac{\xi^2}{4} + \frac{\xi^4}{32}\right)\mathrm{e}^{(-\frac{\xi^2}{4})}\right)\right].\end{aligned} \tag{25}$$

The mean squared and mean absolute displacements are plotted versus the acceptance ratio $P_{\rm acc}$ in one, two and three dimensions in figures 2 and 3. Note that the maximum is shifted to the left, i.e., to the smallest values of the acceptance ratio, when the space dimension increases.

3.2. Uniform radius sampling

The acceptance ratio $P_{{\rm acc},w}$ in D dimensions can be expressed as

$$P_{{\rm acc},w}(\delta) = c_D \int_D \mathrm{d}^D\mathbf{r}\exp(-\beta k\mathbf{r}^2/2)\int_{|h|\leqslant\delta}\mathrm{d}^D\mathbf{h}P_w(h)\min(1, \exp(-\beta k(|\mathbf{r}+\mathbf{h}|^2 - r^2)/2)) \tag{26}$$

where $P_w(h)$ is the weighted probability. For a uniform distribution in radius, $h^{D-1}P_w(h) = (DV_D\delta)^{-1}$. Using the method developed in the above section, it is straightforward to obtain that

$$\frac{\mathrm{d}(\xi P_{{\rm acc},w}(\delta))}{\mathrm{d}\xi} = \left(1 - \mathrm{erf}\left(\frac{\xi}{2}\right)\right) \tag{27}$$

which shows that the acceptance ratio is the same whatever the dimension and explains the data collapse observed in (Bouzida *et al* 1992). Similarly, the generating function $Z(\lambda, \xi)$ can be shown to obey to the differential equation

$$\frac{\partial Z(\lambda, \xi)}{\partial \xi} = \exp\left(-\sqrt{\frac{2}{\beta k}}\lambda\xi\right)\left(1 - \mathrm{erf}\left(\frac{\xi}{2}\right)\right) \tag{28}$$

independently of the dimension D. This proves that $Z(\lambda, \xi)$ and all moments such as $\langle|\Delta r|\rangle$ and $\langle(\Delta r)^2\rangle$ are independent of dimension, as numerically found by BKS (Bouzida *et al* 1992).

4. Dynamic behaviour

In addition to the exact results for the static properties presented above, we have investigated the dynamic behaviour of the SHO by using numerical and analytical approaches. For simplicity, we discuss only the unidimensional case, but the approach can be generalized to D dimensions.

The master equation describing the dynamical evolution of the system during the Monte Carlo simulation, equation (1), can be formally written as

$$\frac{\mathrm{d}\mathbf{P}(t)}{\mathrm{d}t} = -L\mathbf{P}(t) \tag{29}$$

where L is a linear operator acting on P and the Metropolis rule, equation (4), is used for the transition rate. We consider the spectrum of eigenvalues λ of L. Denoting by $P_\lambda(x)$ the eigenfunction associated with λ and introducing $f_\lambda(x)$ via $P_\lambda(x) = P_{\mathrm{eq}}(x)\, f_\lambda(x)$, where $P_{\mathrm{eq}}(x)$ is given in equation (3), one can express the eigenvalue equation

$$\lambda P_{\mathrm{eq}}(x)\, f_\lambda(x) = L(P_{\mathrm{eq}}(x)\, f_\lambda(x)) \tag{30}$$

as

$$\lambda f_\lambda(x) = \frac{1}{2\delta}\int_{-\delta}^{\delta} \mathrm{d}h\, \mathrm{Min}(1, \mathrm{e}^{-\beta(V(x+h)-V(x))})(f_\lambda(x) - f_\lambda(x+h)). \tag{31}$$

Multiplying both sides by $\exp(-\beta V(x))\, f_\lambda^*(x)$, where the star denotes a complex conjugate, and integrating over x then gives

$$\lambda = \frac{1}{4\delta}\frac{\int_{-\infty}^{+\infty}\mathrm{d}x\int_{-\delta}^{\delta}\mathrm{d}h\, \mathrm{Min}(\mathrm{e}^{-\beta V(x)}, \mathrm{e}^{-\beta V(x+h)})|f_\lambda(x+h) - f_\lambda(x)|^2}{\int_{-\infty}^{+\infty}\mathrm{d}x\, \mathrm{e}^{-\beta V(x)}|f_\lambda(x)|^2}. \tag{32}$$

As anticipated for a Markov process satisfying detailed balance, one deduces from the above formula that all eigenvalues are real and positive; the smallest eigenvalue is $\lambda_0 = 0$ and it is associated with $f_0(x) = \text{constant} \neq 0$. One needs to consider only real eigenfunctions. Moreover, the eigenvalues can be sorted according to the symmetry of the associated eigenfunctions: it is easy to check that the eigenfunctions are either even or odd functions of x, due to the fact that the potential $V(x)$ is an even function of x.

Any solution of the master equation can be expanded as

$$P(x,t) = P_{\mathrm{eq}}(x)\left(1 + \sum_{\lambda>0} c_\lambda f_\lambda(x)\, \mathrm{e}^{-\lambda t}\right) \tag{33}$$

and a similar expansion applies to the conditional probability $P(x,t|x_0,0)$ from which one can compute any time-dependent correlation function. The long-time kinetics governing the approach to equilibrium in $P(x,t)$ and in any correlation function is characterized by the smallest non-zero eigenvalue for which the amplitude, i.e., the projection of $P(x,0)$, or of the dynamic observable, onto the relevant eigenfunction, does not vanish.

Since, according to equation (32), the eigenvalues are expressed as the ratio of two positive quadratic functionals (that in the denominator being also definite), one can use the Rayleigh—Ritz procedure to find a variational upper bound for the eigenvalues (Dettman 1962, Arfken 1985). Consider first the smallest non-zero eigenvalue λ_1. For any real function $\phi(x)$ which is both normalized and orthogonal to $f_0(x)$, i.e., satisfies

$$\int_{-\infty}^{\infty} P_{\mathrm{eq}}(x)\phi(x)^2\, \mathrm{d}x = 1 \tag{34}$$

$$\int_{-\infty}^{\infty} P_{\mathrm{eq}}(x)\phi(x)\, \mathrm{d}x = 0 \tag{35}$$

one has the inequality

$$\lambda_1 \leqslant \lambda_1[\phi] = \frac{1}{4\delta}\int_{-\infty}^{+\infty} \mathrm{d}x \int_{-\delta}^{\delta} \mathrm{d}h \,\mathrm{Min}(\mathrm{e}^{-\beta V(x)}, \mathrm{e}^{-\beta V(x+h)})|\phi(x+h)-\phi(x)|^2. \tag{36}$$

A convenient choice of trial functions is provided by linear combinations of Hermite polynomials $H_n(\xi)$ (where, as in the previous sections $\xi = \sqrt{\frac{\beta k}{2}}\delta$), with $n > 0$, since these form, up to a trivial multiplicative factor, an orthonormal basis with respect to the weight function $\exp(-\beta V(x))$ with $V(x) = (1/2)kx^2$. For λ_1, which is associated with an odd eigenfunction, one needs to consider only the odd polynomials $H_{2n+1}(\xi)$, $n \geqslant 0$.

The simplest estimate of λ_1 is provided by taking

$$\phi(\xi) = \frac{H_1(\xi)}{\sqrt{2\sqrt{\pi}}} = \sqrt{\frac{2}{\sqrt{\pi}}}\xi \tag{37}$$

which gives

$$\lambda_1[\phi] = \frac{4}{3}\left[\frac{\xi^2}{4}\left(1-\mathrm{erf}\left(\frac{\xi}{2}\right)\right) + \frac{2}{\sqrt{\pi}\xi}\left(1-\left(1+\frac{\xi^2}{4}\right)\exp\left(\frac{-\xi^2}{4}\right)\right)\right]. \tag{38}$$

With this choice of $\phi(\xi)$, $\lambda_1[\phi]$ simply reduces to the mean squared displacement $\langle(\Delta x)^2\rangle$ multiplied by $\left(\frac{\beta k}{2}\right)$ (see equation (15)). One then derives from section 2 that $\lambda_1[\phi]$ versus ξ passes though a maximum for $\xi \simeq 2.611\,648$, which corresponds to an acceptance ratio of $P_{\mathrm{acc}} = 0.417\,67$.

A better estimate of λ_1 can be obtained by using a linear combination of $H_1(\xi)$ and $H_3(\xi)$:

$$\phi(\xi;\theta) = \left[\frac{\cos(\theta)}{\sqrt{2\sqrt{\pi}}}H_1(\xi) + \frac{\sin(\theta)}{\sqrt{48\sqrt{\pi}}}H_3(\xi)\right] \tag{39}$$

where only one independent parameter θ appears due to the normalization condition. The best bound is determined by minimizing the expression $\lambda_1[\phi]$ with respect to θ:

$$\frac{\partial\lambda_1[\phi]}{\partial\theta} = 0. \tag{40}$$

The result is a lengthly algebraic formula that is plotted in figures 4 and 5, together with the expression in equation (38).

An improved estimate of λ_1 can be derived by noting that at large ξ, λ_1 is inversely proportional to ξ. Actually, one can show that this is true for all eigenvalues except $\lambda_0 = 0$. By considering equation (31) in the limit where x goes to zero, one arrives at the result (see appendix B)

$$\lambda(\xi) \sim \frac{\sqrt{\pi}}{2\xi} + O(\mathrm{e}^{-\xi^2}) \tag{41}$$

valid for large ξ. Note that the correction terms are very small as soon as $\xi \geqslant 3$. One can build an estimate of $\lambda_1(\xi)$ by using the piecewise function that is equal to $\frac{\sqrt{\pi}}{2\xi}$ for $\xi \geqslant \xi^*$ and is equal to $\lambda_1[\phi]$ obtained for a linear combination of H_1 and H_3 (see above) for $\xi \leqslant \xi^*$, where ξ^* is the value at which $\lambda_1[\phi] = \frac{\sqrt{\pi}}{2\xi}$. $\lambda(\xi)$ is then maximum for $\xi = \xi^* \simeq 2.35$; the corresponding value of the acceptance ratio is $P_{\mathrm{acc}} \simeq 0.56$. The estimate is shown in figures 4 and 5.

In order to compare our results with the BKS paper (Bouzida *et al* 1992), it is necessary to calculate the second eigenvalue λ_2. The trial function is then chosen in a subspace orthogonal not only to $f_0(\xi) =$ constant but also to the eigenfunction associated with λ_1. A convenient choice is provided by (normalized) linear combinations of the even Hermite polynomials

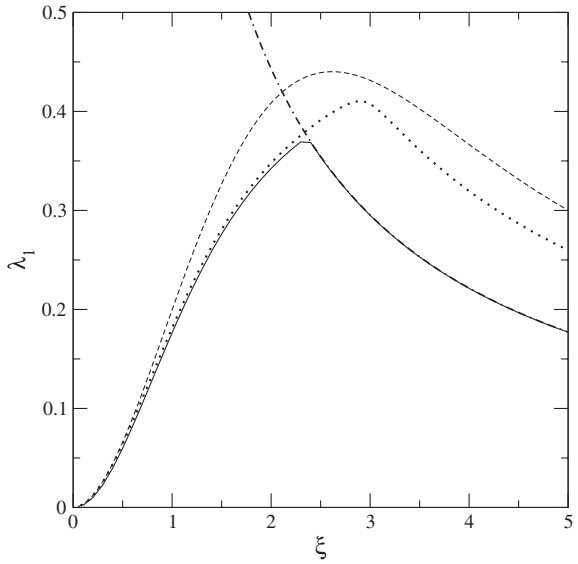

Figure 4. λ_1 versus ξ . The full curve was obtained by numerical diagonalization of the master equation. The dashed curve corresponds to the zeroth-order estimate, equation (38), the dotted curve corresponds to the solution of the first-order trial function, equation (40)), and the dash-dot curve corresponds to the exact asymptotic behaviour, equation (41).

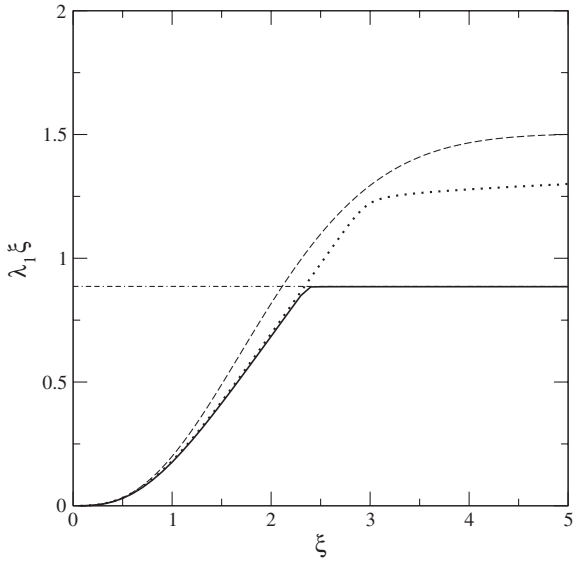

Figure 5. Same as figure 4 except $\xi\lambda_1$ versus ξ.

$H_{2n}(\xi)$ with $n \geqslant 1$. An estimate of λ_2 can be obtained by using a linear combination of $H_2(\xi)$ and $H_4(\xi)$:

$$\phi(\xi;\theta) = \left[\frac{\cos(\theta)}{2\sqrt{2\sqrt{\pi}}}H_2(\xi) + \frac{\sin(\theta)}{8\sqrt{6\sqrt{\pi}}}H_4(\xi)\right] \tag{42}$$

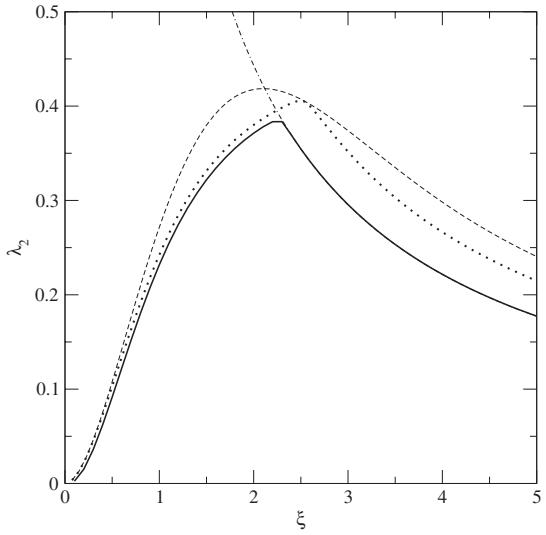

Figure 6. λ_2 versus ξ . The full curve was obtained by numerical diagonalization of the master equation. The dashed curve corresponds to the zeroth-order estimate, ($\theta = 0$ in equation (42)), the dotted curve corresponds to the solution of the first-order trial function, equation (42) and the dash-dot curve corresponds to the exact asymptotic behaviour, equation (41).

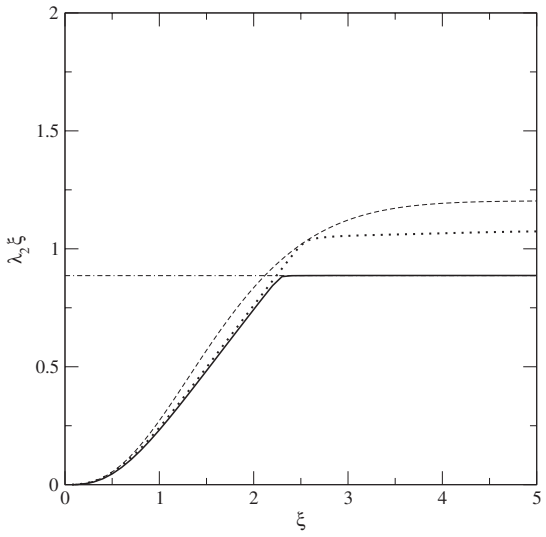

Figure 7. Same as figure 6 except $\xi\lambda_2$ versus ξ.

and the result is shown in figures 6 and 7, together with the zeroth-order approximation obtained with only $H_2(\xi)$ and the improved estimate taking into account the large-ξ behaviour.

In addition to the above analytical estimates, we have also performed a numerical study of the spectrum of eigenvalues of the master equation (1). The latter has been discretized in x-space by taking a constant step size Δ, which leads to a matrix form

$$\frac{\mathrm{d}\mathbf{P}(t)}{\mathrm{d}t} = -\mathbf{W}\mathbf{P}(t) \tag{43}$$

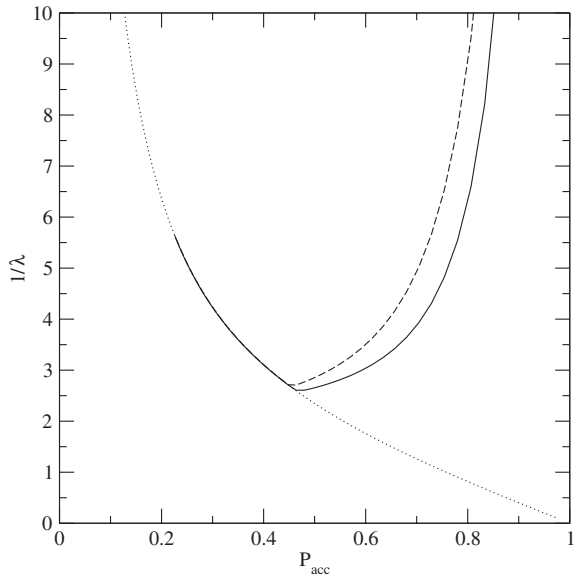

Figure 8. Inverse of the first non-zero eigenvalues, $1/\lambda_1$ (dashed curve), $1/\lambda_2$ (full curve), and asymptotic behaviour (dotted curve) versus the acceptance probability $P_{\rm acc}$

where $\mathbf{P}$ is a vector with components $P_i(t) = P(x_i, t)$ and the elements W_{ij} of the matrix $\mathbf{W}$ are such that

$$W_{ii} = \Delta \sum_{j=i-Nh,\, j\neq i}^{i+Nh} W(i \to j) \qquad W_{ij} = -\Delta W(j \to i) \tag{44}$$

and $W(i \to j) = \mathrm{Min}(1, \mathrm{e}^{-\beta(V(x_j)-V(x_i))})$. The eigenvalues λ can then be obtained via an exact numerical diagonalization of the matrix W. In practice, convergence is obtained for a unidimensional lattice of 400 sites, where the x-range is $[-10, 10]$, and ξ goes from 0 to 5. One checks that the lowest eigenvalue is equal to zero and corresponds to the equilibrium state, and that all other eigenvalues are real and strictly positive and behave as $\sqrt{\pi}/(2\xi)$ for large enough ξ. The results for the first non-zero eigenvalue λ_1 and λ_2 are displayed in figures 4 and 6, respectively. One can see that the best analytical estimate described above (linear combination of two Hermite polynomials plus exact asymptotic behaviour at large ξ) is in excellent agreement with the numerical value in both cases.

The above analysis allows us to derive by analytical means the simulation result obtained by BKS (Bouzida *et al* 1992) for the dependence of the characteristic time τ of the energy–energy correlation function on the acceptance ratio: approximating τ by $1/\lambda_2$ (since the energy $V(x)$ is an even function of x, its projection on the first eigenfunction associated with λ_1 vanishes), using for λ_2 our best analytical estimate, and combining this with the exact result for the acceptance ratio $P_{\rm acc}$ in section 2 lead to the full curve plotted in figure 8; the time τ is minimum for the acceptance ratio close to 0.47, as found by BKS (Bouzida *et al* 1992) ($\simeq 0.50$).

In figure 8, we have also plotted $1/\lambda_1$ versus the acceptance ratio: it is minimum for $P_{\rm acc} = 0.45$. Note that using the results of this and the preceding sections, one can rigorously show that the correlation time τ, no matter how it is precisely defined, diverges as $1/P_{\rm acc}$ when $P_{\rm acc} \to 0$ and as $1/(1 - P_{\rm acc})$ when $P_{\rm acc} \to 1$.

In summary, we have shown that the spectrum of the master equation is very accurately described for small and intermediate displacements by a trial eigenfunction composed of two Hermite polynomials. When combined with the exact asymptotic result obtained by the analysis of the master equation, we obtain a complete description of the dynamics.

5. Conclusion

We have obtained exact results concerning Metropolis algorithms for the displacement of a particle in the simple harmonic potential. Our analysis provides a theoretical explanation of the numerical results obtained by BKS (Bouzida *et al* 1992). In particular, we show that the results become independent of the space dimension when the successive trial moves are sampled according to a Metropolis algorithm with a uniform distribution in radius (instead of volume). This rationalizes the search for efficient Monte Carlo methods for the simulation of systems with intrinsic inhomogeneity and anisotropy such as biological molecules (Bouzida *et al* 1992, Swendsen 2002).

To our knowledge, the analytical expressions obtained here for both the static and dynamic properties are among the very few exact results available on Monte Carlo methods. They can be taken as a starting point for perturbative studies of more complex models, but generalization to systems with many coupled degrees of freedom is still out of reach.

Acknowledgment

J T acknowledges support from the National Science Foundation (Grant No CHE-9814236).

Appendix A. Acceptance probability

The derivation of equation (21) can be done from equation (20) after some manipulations whose details are given here. Let us denote I_D and J_D as

$$I_D = \int_0^{\xi/2} \mathrm{d}v\, v^{D-1}\, \mathrm{e}^{-v^2} \int_{-1}^{1} \mathrm{d}u\, (1-u^2)^{(D-3)/2} \exp(-(\xi^2 + 2\xi v u)) \tag{A.1}$$

$$J_D = \int_{\xi/2}^{+\infty} \mathrm{d}v\, v^{D-1}\, \mathrm{e}^{-v^2} \left[\int_{-1}^{-\xi/(2v)} \mathrm{d}u\, (1-u^2)^{(D-3)/2} + \int_{-\xi/(2v)}^{1} \mathrm{d}u\, (1-u^2)^{(D-3)/2} \exp((-(\xi^2 + 2\xi v u))) \right]. \tag{A.2}$$

Changing the variable u to $y = vu$ and v to $t = v^2 - y^2$ leads to the following relations:

$$I_D = \int_0^{\xi/2} \mathrm{d}y \frac{\exp(-(\xi+y)^2) + \exp(-(y-\xi)^2)}{2} \int_0^{\xi^2/4-y^2} \mathrm{d}t\, t^{(D-3)/2}\, \mathrm{e}^{-t} \tag{A.3}$$

$$J_D = \int_{\xi/2}^{+\infty} \mathrm{d}y \frac{\exp(-y^2)}{2} \int_0^{+\infty} \mathrm{d}t\, t^{(D-3)/2}\, \mathrm{e}^{-t} + \int_0^{\xi/2} \mathrm{d}y \frac{\exp(-(y-\xi)^2)}{2} \int_{\xi^2/4-y^2}^{+\infty} \mathrm{d}t\, t^{(D-3)/2}\, \mathrm{e}^{-t}$$

$$+\int_0^{\xi/2} \mathrm{d}y \frac{\exp(-(y+\xi)^2)}{2} \int_{\xi^2/4-y^2}^{+\infty} \mathrm{d}t\, t^{(D-3)/2}\, \mathrm{e}^{-t}$$
$$+\int_{\xi/2}^{+\infty} \mathrm{d}y \frac{\exp(-(y+\xi)^2)}{2} \int_0^{+\infty} \mathrm{d}t\, t^{(D-3)/2}\, \mathrm{e}^{-t}. \tag{A.4}$$

Using that $\int_0^{+\infty} \mathrm{d}t\, t^{(D-3)/2}\, \mathrm{e}^{-t} = \Gamma((D-1)/2)$, one obtains that

$$I_D + J_D = \frac{\sqrt{\pi}}{2}\Gamma\left(\frac{D-1}{2}\right)\left(1 - \mathrm{erf}\left(\frac{\xi}{2}\right)\right). \tag{A.5}$$

Inserting equations (A.5) in equation (20) leads to equation (21).

Appendix B. Asymptotic behaviour of the eigenvalues for large δ

Consider equation (31) in the limit $x \to 0$; one obtains after rearranging the various terms:

$$\lambda f_\lambda(x) = \frac{1}{2\delta}\int_{-\delta}^{\delta} \mathrm{d}h \exp\left(\frac{-\beta k}{2}((x+h)^2 - x^2)\right)(f_\lambda(x) - f_\lambda(x+h))$$
$$+\frac{1}{2\delta}\int_{-2x}^{0} \mathrm{d}h \left(1 - \exp\left(\frac{-\beta k}{2}((x+h)^2 - x^2)\right)\right)(f_\lambda(x) - f_\lambda(x+h)). \tag{B.1}$$

The second term of the right-hand side of equation (B.1) is at most of order $x^3|f_\lambda(x)|$ and is always negligible so that one can rewrite equation (B.1) as

$$\left(\lambda\delta - \int_0^{\delta} \mathrm{d}h\, \mathrm{e}^{\frac{-\beta k}{2}h^2} + O(x^2)\right) f_\lambda(x) \simeq -\frac{\mathrm{e}^{\frac{-\beta k}{2}x^2}}{2}\int_{-\delta}^{\delta} \mathrm{d}h \exp\left(\frac{-\beta k}{2}(x+h)^2\right) f_\lambda(x+h). \tag{B.2}$$

Shifting the variable from h to $x+h$ in the integral of the rhs of equation (B.2) and using the orthogonality of $f_\lambda(x)$ to $f_0(x) =$ constant for all non-zero eigenvalues λ, i.e., $\int_{-\infty}^{+\infty} \mathrm{d}x \exp\left(\frac{-\beta k}{2}x^2\right) f_\lambda(x) = 0$, leads to the following expression,

$$\left(\lambda\delta - \sqrt{\frac{\pi}{2\beta k}} + O(x^2)\right) f_\lambda(x) \simeq \frac{1+O(x^2)}{2}\left[\int_{x+\delta}^{+\infty} \mathrm{d}h\, \mathrm{e}^{\frac{-\beta k h^2}{2}} f_\lambda(h) + \int_{-\infty}^{x-\delta} \mathrm{d}h\, \mathrm{e}^{\frac{-\beta k h^2}{2}} f_\lambda(h)\right] \tag{B.3}$$

for any non-zero λ. The rhs of equation (B.3) can be Taylor expanded, which gives

$$\left(\lambda\delta - \sqrt{\frac{\pi}{2\beta k}} + O(x^2)\right) f_\lambda(x) \simeq \frac{1}{2}\left[\int_{\delta}^{+\infty} \mathrm{d}h\, \mathrm{e}^{\frac{-\beta k h^2}{2}}(f_\lambda(h) + f_\lambda(-h))\right.$$
$$\left. - x\, \mathrm{e}^{\frac{-\beta k h^2}{2}}(f_\lambda(h) - f_\lambda(-h)) + O(x^2)\right]. \tag{B.4}$$

If the eigenfunction f_λ is an even function of x, one then derives that $f_\lambda(x) = f_\lambda(0) + O(x^2)$ with $f_\lambda(0) \neq 0$ and

$$\left(\lambda\delta - \sqrt{\frac{\pi}{2\beta k}}\right) = \int_{\delta}^{+\infty} \mathrm{d}h \exp\left(\frac{-\beta k h^2}{2}\right)\frac{f_\lambda(h)}{f_\lambda(0)} \tag{B.5}$$

which after introducing $\xi = \sqrt{\frac{\beta k}{2}}\delta$ can be rewritten as

$$\lambda = \frac{\sqrt{\pi}}{2\xi} + \sqrt{\frac{2}{\beta k}}\int_{\xi}^{+\infty} \mathrm{d}h \exp\left(\frac{-\beta k h^2}{2}\right)\frac{f_\lambda\left(\sqrt{\frac{2}{\beta k}}h\right)}{f_\lambda(0)}. \tag{B.6}$$

If the eigenfunction is an odd function of x, one has that $f_\lambda(x) = f'_\lambda(0)x(1 + O(x^2)$ with $f'_\lambda(0) \neq 0$ and

$$\lambda = \frac{\sqrt{\pi}}{2\xi} \frac{f_\lambda\left(\sqrt{\frac{2}{\beta k}}\xi\right)}{f_\lambda(0)} \exp(-\xi^2). \tag{B.7}$$

From equations (B.6) and (B.7), one immediately obtains that all non-zero eigenvalues behave as

$$\lambda \sim \frac{\sqrt{\pi}}{2\xi} + O(\exp(-\xi^2)) \tag{B.8}$$

when $\xi \to +\infty$, since $f_\lambda(x)$ diverges more slowly than e^{x^2} when $x \to +\infty$.

References

Allen M P and Tildesley D J 1987 *Computer Simulation of Liquids* (London: Clarendon)

Arfken G 1985 *Mathematical Methods for Physicists* 3rd edn (Orlando, FL: Academic)

Binder K 1997 Applications of Monte-Carlo methods to statistical physics *Rep. Prog. Phys.* **60** 487

Bouzida D, Kumar S and Swendsen R 1992 Efficient Monte Carlo methods for the computer simulation of biological molecules *Phys. Rev.* A **45** 8894

Dettman J 1962 *Mathematical Methods in Physics and Engineering* (New York: Dover)

Frenkel D and Smit B 2002 *Understanding Molecular Simulation: from Algorithms to Applications* (San Diego: Academic)

Kolafa J 1988 On optimization of Monte Carlo simulations *Mol. Phys.* **63** 559

Mountain R and Thirumalai D 1994 Quantitative measure of efficiency of Monte Carlo simulations *Physica* A **210** 453

Swendsen R 2002 Private communication